The novel product of a five-exon *stargazin*-related gene abolishes Ca$_V$2.2 calcium channel expression

Fraser J.Moss, Patricia Viard, Anthony Davies, Federica Bertaso, Karen M.Page, Alex Graham, Carles Cantí, Mary Plumpton[1], Christopher Plumpton[2], Jeffrey J.Clare[2] and Annette C.Dolphin[3]

Department of Pharmacology, University College London, Gower Street, London WC1E 6BT and [2]Gene Expression and Protein Biochemistry, and [1]Bioinformatics Unit, GlaxoSmithKline, Medicines Research Center, Gunnels Wood Road, Stevenage, Herts SG1 2NY, UK

[3]Corresponding author
e-mail: a.dolphin@ucl.ac.uk

P.Viard, A.Davies and F.Bertaso contributed equally to this work

We have cloned and characterized a new member of the voltage-dependent Ca^{2+} channel γ subunit family, with a novel gene structure and striking properties. Unlike the genes of other potential γ subunits identified by their homology to the *stargazin* gene, *CACNG7* is a five-, and not four-exon gene whose mRNA encodes a protein we have designated γ$_7$. Expression of human γ$_7$ has been localized specifically to brain. N-type current through Ca$_V$2.2 channels was almost abolished when co-expressed transiently with γ$_7$ in either *Xenopus* oocytes or COS-7 cells. Furthermore, immunocytochemistry and western blots show that γ$_7$ has this effect by causing a large reduction in expression of Ca$_V$2.2 rather than by interfering with trafficking or biophysical properties of the channel. No effect of transiently expressed γ$_7$ was observed on pre-existing endogenous N-type calcium channels in sympathetic neurones. Low homology to the stargazin-like γ subunits, different gene structure and the unique functional properties of γ$_7$ imply that it represents a distinct subdivision of the family of proteins identified by their structural and sequence homology to stargazin.
Keywords: calcium channel/expression/γ subunit/ stargazin/suppression

Introduction

Voltage-dependent calcium channels (VDCCs) play a fundamental role in the coupling of membrane depolarization to many cellular processes by regulating cytoplasmic Ca^{2+} concentration in excitable cells. They are heteromultimers consisting of a pore-forming α$_1$ subunit assembled with auxiliary β, α2δ and possibly γ subunits. These subunits can be encoded by several different genes with alternative splice variants and are expressed in a tissue-specific manner. Much work has concentrated on the characterization of functional properties of the α$_1$, β and α2δ subunits (Birnbaumer *et al*., 1998; Dolphin, 1998; Jones, 1998; Perez-Reyes, 1998; Catterall, 2000). However, research concerning the role of the γ subunit has not been as extensive.

Until recent years, only a single gene, exclusively expressed in skeletal muscle, was believed to encode a VDCC γ subunit (Jay *et al*., 1990; Powers *et al*., 1993). Recordings of Ca^{2+} currents from dihydropyridine receptors (DHPRs) of skeletal myotubes from mice lacking this γ$_1$ subunit suggest that its role is to limit calcium entry through these channels, increase the rate at which the channels inactivate and hyperpolarize the half-maximal potential for the voltage dependence of steady-state inactivation (Freise *et al*., 2000; Ahern *et al*., 2001). Subsequently, a second putative VDCC γ subunit, γ$_2$, was identified based on its structural similarity to γ$_1$, despite having only weak protein sequence identity (25%) (Letts *et al*., 1998). Mutations in the γ$_2$ gene, *cacng2*, were found to underlie the absence epilepsy phenotype of the allelic stargazer (*stg*) and waggler (*wag*) mutant mice. Subsequent studies have identified six further putative γ subunits (γ$_3$–γ$_8$), not all of which have been cloned and expressed (Black and Lennon, 1999; Burgess *et al*., 1999, 2001; Klugbauer *et al*., 2000).

The γ$_2$, γ$_3$ and γ$_4$ subunits form a subfamily exclusively localized to the central nervous system (CNS) (Letts *et al*., 1998; Klugbauer *et al*., 2000) whose interaction with VDCCs has been investigated in several studies (Letts *et al*., 1998; Klugbauer *et al*., 2000; Kang *et al*., 2001; Sharp *et al*., 2001). The γ$_5$ and γ$_7$ subunits (Burgess *et al*., 1999, 2001) are predicted to represent another subfamily of stargazin-related proteins, with extremely low sequence identity to γ$_1$ and ~25% identity to γ$_2$. These subunits, like other members of the putative γ subunit superfamily, are proteins predicted to have four transmembrane segments with intracellular N- and C-termini, and were reported to be encoded by a gene assembled from four exons (Burgess *et al*., 2001). However, assembly of the full-length γ$_5$ and γ$_7$ cDNAs has not been described and there are no functional data for either of these γ subunits.

In the present study, we report the identification, cloning and functional characterization of a novel protein we have named the γ$_7$ subunit. The first four exons of the gene encoding this protein are identical to those encoding the predicted γ$_7$ subunit gene previously described by Burgess *et al*. (2001), but the transcription and translation of a final fifth exon results in the γ$_7$ described in the present study having a very different and much longer C-terminus. Our results show that the co-expression of the γ$_7$ subunit almost abolishes the functional expression and markedly suppresses the level of Ca$_V$2.2 subunit protein. We also report the identification of the γ$_5$ subunit which, like γ$_7$, is predicted to be encoded by a five-exon gene.

Results

Cloning of the γ₅ and γ₇ genes

The full-length mouse *stargazin* sequence (Letts *et al.*, 1998) was used as a query sequence to search the DNA databases. A short 487 bp sequence was assembled from three expressed sequence tags (ESTs) and was found to contain an open reading frame (ORF) with 26% identity to *stargazin*, although it contained no in-frame start or stop codons.

A 487 bp fragment corresponding to this *in silico* sequence was amplified from human whole brain cDNA, and sequence analysis confirmed the computer predictions. Primers specific for each end of this fragment were used to amplify the missing parts of the ORF using 5′ and 3′ RACE. A 330 bp fragment containing the missing 5′ sequence and start ATG codon, and a 400 bp band containing the missing 3′ sequence and stop codon were obtained. These three DNA fragments were then used to assemble the full-length 828 bp *stargazin*-like ORF in a single 'splice-overlap' PCR.

When this full-length sequence was used to search the human high-throughput genomic sequences (HTGS) using the BLASTn algorithm, a bacterial artificial chromosome (BAC), clone AC008440, derived from human chromosome 19 was identified. Analysis of this BAC using the gene prediction program Genscan (Burge and Karlin, 1997) predicts that the 828 bp ORF is assembled from five exons and encodes a 275 amino acid protein.

When compared with all of the previously published γ subunits, this 828 bp cDNA clone exhibited 100% identity to the previously predicted human γ₇ subunit over the first four exons (Burgess *et al.*, 2001). However, the sequence of the cDNA clone described here diverges from the γ₇ sequence (Burgess *et al.*, 2001), due to the presence of the fifth exon (Figure 1A and B). It would therefore appear that *CACNG7* is in fact a five-exon gene that encodes the γ₇ subunit, and the previously predicted four-exon γ₇ sequence results from read-through into intron four (Figure 1B).

BLAST searches of mouse HTGS identified *cacng7*, the mouse orthologue of the γ₇ gene within BAC AC079557, which, like its human counterpart, contained five exons. Confirmation that the mouse γ₇ mRNA is expressed was obtained by amplifying the complete cDNA in a single RT–PCR from mouse cerebellar total RNA. The mouse orthologue possesses 70% identity to the human γ₇ at the nucleic acid level and, remarkably, 100% identity at the protein level.

BLASTn searches and Genscan analysis of human chromosome 17 BAC AC005988 identified another related gene encoding a 275 amino acid protein. This gene also possessed five exons and predicted a protein with 70.5% amino acid identity compared with the human γ₇ and 27% identity compared with human γ₂. It exhibited 100% identity to the previously described human γ₅ subunit (Burgess *et al.*, 1999) over its first 190 amino acids but, like the γ₇ subunit, the additional fifth exon encodes an alternative C-terminus. Unlike the previously predicted four-exon γ₅ and γ₇, the C-termini of the five-exon γ₅ and γ₇ share considerable identity (80%, Figure 1A). We therefore named this subunit γ₅ (gene *CACNG5*) and subsequently identified the mouse orthologue on mouse

chromosome 16 BAC AC079424. The mouse orthologue (*cacng5*) exhibited 89.5% identity at the nucleotide level and 97% identity at the protein level to the human sequence.

Hydropathy plots predict that, like all the stargazin-related proteins, γ₇ and γ₅ have four transmembrane-spanning α-helices with predicted intracellular N- and C-termini (Figure 1C). The final transmembrane-spanning α-helices of γ₇ and γ₅ are predicted to be six and eight amino acids longer, respectively, than their equivalents in the previously predicted four-exon γ₇ or γ₅, and the full-length γ₇ has a much more substantial cytosolic C-terminus than in the predicted four-exon γ₇, in which only four intracellular amino acids are predicted after the final transmembrane segment.

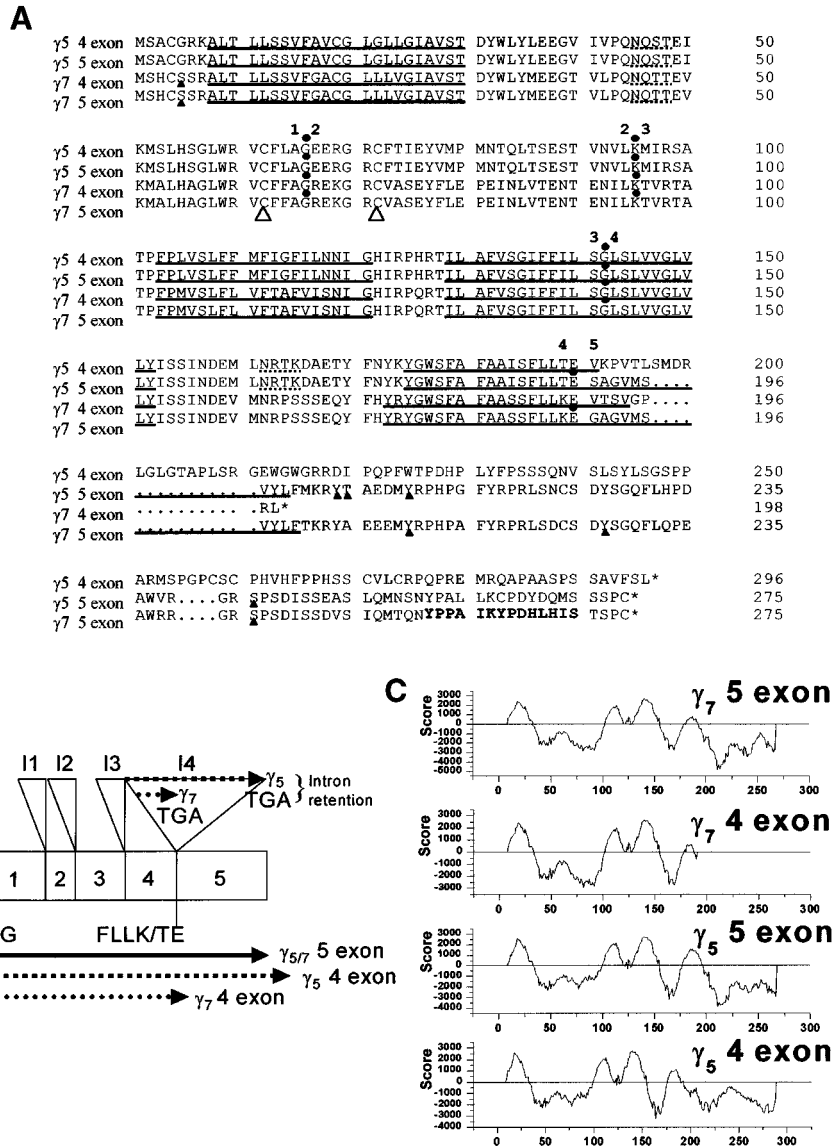The sequences have been deposited in the DDBJ/EMBL/GenBank database with the following accession Nos: human γ₇ (AF458897), human γ₅ (AF458898), mouse γ₇ (AF458899) and mouse γ₅ (AF458900).

Tissue distribution

The tissue distribution of the novel γ₇ mRNA was analysed by northern blot. Figure 2 shows a human multiple tissue northern blot (Figure 2A) and two brain region blots (Figure 2B and C) hybridized with a probe corresponding to nucleotides 576–763 of the γ₇ ORF. This region was chosen because it contains the least identity when compared with other γ-subunits (53% to human γ₂), and is unique to γ₇. Thus, this probe will not detect the predicted four-exon γ₇, should this be expressed. This γ₇-specific probe reveals two transcripts of ~2.4 and 3.0 kb, both of which are expressed only in brain. Both of these transcripts are expressed in all brain regions probed, although the shorter transcript is expressed at greater levels in several areas including cerebellum, amygdala, hippocampus and thalamus. These blots were stripped and re-probed using the same probe as that designed to detect the four-exon γ₇ (Burgess *et al.*, 2001). This probe, corresponding to nucleotides 80–482 of the γ₇ ORF, would detect both the predicted four-exon γ₇ and full-length γ₇ transcripts. No additional transcripts were seen in any of the blots with this probe. Indeed, precisely the same expression profile was seen as with the full-length γ₇-specific probe, including the same differential expression of the short and long transcripts seen in cerebellum, amygdala, hippocampus and thalamus (data not shown).

Influence of the γ₇ subunit on heterologous expression of VDCCs and K_V3.1b

Having investigated the tissue distribution of the γ₇ subunit in human brain, we next examined the effect of expression of this protein on Ba^{2+} currents recorded from neuronal VDCCs expressed in COS-7 cells. For comparison with immunocytochemistry data (see below), we transfected an N-terminal green fluorescent protein-tagged Ca_V2.2 construct (GFP–Ca_V2.2), previously shown to have no significant differences in its biophysical properties compared with the non-tagged channel (Raghib *et al.*, 2001). These experiments revealed an almost total abolition of whole-cell GFP–Ca_V2.2 Ba^{2+} current (I_{Ba}) in cells co-transfected with γ₇ (Figure 3A, upper trace). In 1 mM Ba^{2+}, mean current density of cells expressing GFP–Ca_V2.2/β_{1b}/α2δ₂ was –13.5 ± 4.3 pA/pF at 0 mV (*n* = 20) (Figure 3B)

A

```
           1 2                              2 3
γ5 4 exon  MSACGRKALT LLSSVFAVCG LGLLGIAVST DYWLYLEEGV IVPQNQSTEI   50
γ5 5 exon  MSACGRKALT LLSSVFAVCG LGLLGIAVST DYWLYLEEGV IVPQNQSTEI   50
γ7 4 exon  MSHCSSRALT LLSSVFGACG LLLVGIAVST DYWLYMEEGT VLPQNQTTEV   50
γ7 5 exon  MSHCSSRALT LLSSVFGACG LLLVGIAVST DYWLYMEEGT VLPQNQTTEV   50

γ5 4 exon  KMSLHSGLWR VCFLAGEERG RCFTIEYVMP MNTQLTSEST VNVLKMIRSA  100
γ5 5 exon  KMSLHSGLWR VCFLAGEERG RCFTIEYVMP MNTQLTSEST VNVLKMIRSA  100
γ7 4 exon  KMALHAGLWR VCFFAGREKG RCVASEYFLE PEINLVTENT ENILKTVRTA  100
γ7 5 exon  KMALHAGLWR VCFFAGREKG RCVASEYFLE PEINLVTENT ENILKTVRTA  100
                      △            △

                                            3 4
γ5 4 exon  TPFPLVSLFF MFIGFILNNI GHIRPHRTIL AFVSGIFFIL SGLSLVVGLV  150
γ5 5 exon  TPFPLVSLFF MFIGFILNNI GHIRPHRTIL AFVSGIFFIL SGLSLVVGLV  150
γ7 4 exon  TPFPMVSLFL VFTAFVISNI GHIRPQRTIL AFVSGIFFIL SGLSLVVGLV  150
γ7 5 exon  TPFPMVSLFL VFTAFVISNI GHIRPQRTIL AFVSGIFFIL SGLSLVVGLV  150

                                  4 5
γ5 4 exon  LYISSINDEM LNRTKDAETY FNYKYGWSFA FAAISFLLTE VKPVTLSMDR  200
γ5 5 exon  LYISSINDEM LNRTKDAETY FNYKYGWSFA FAAISFLLTE SAGVMS....  196
γ7 4 exon  LYISSINDEV MNRPSSSEQY FHYRYGWSFA FAASSFLLKE VTSVGP....  196
γ7 5 exon  LYISSINDEV MNRPSSSEQY FHYRYGWSFA FAASSFLLKE GAGVMS....  196

γ5 4 exon  LGLGTAPLSR GEWGWGRRDI PQPFWTPDHP LYFPSSSQNV SLSYLSGSPP  250
γ5 5 exon  .......... VYLFMKRYT AEDMYRPHPG FYRPRLSNCS DYSGQFLHPD  235
γ7 4 exon  .......... .RL*                                         198
γ7 5 exon  .......... VYLETKRYA EEEMYRPHPA FYRPRLSDCS DYSGQFLQPE  235

γ5 4 exon  ARMSPGPCSC PHVHFPPHSS CVLCRPQPRE MRQAPAASPS SAVFSL*      296
γ5 5 exon  AWVR....GR SPSDISSEAS LQMNSNYPAL LKCPDYDQMS SSPC*        275
γ7 5 exon  AWRR....GR SPSDISSDVS IQMTQNYPPA IKYPDHLHIS TSPC*        275
```
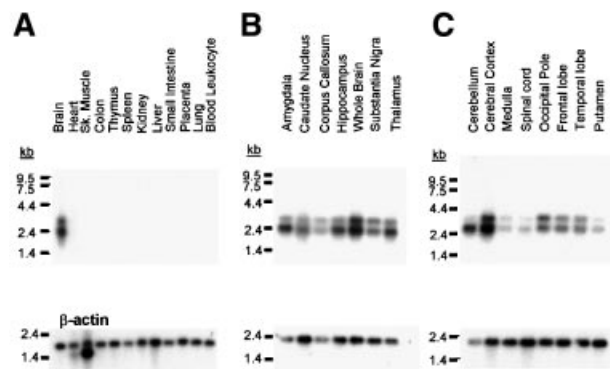
B

C

Fig. 1. Protein sequences, proposed splicing mechanism and hydropathy plots of a family of low homology *stargazin*-related genes. (**A**) Alignment of the five-exon γ_5 and γ_7 subunit sequences with the previously predicted four-exon γ_5 and γ_7 subunits using the Clustal_W algorithm. Dotted lines indicate consensus *N*-glycosylation sites and solid triangles beneath residues mark consensus sites for phosphorylation by cAMP- and cGMP-dependent protein kinase, protein kinase C, casein kinase II or tyrosine kinase. The exon–intron boundaries are marked by solid dots above the residue whose codon is interrupted by the adjacent intron. Note that the sequence identity between γ_5 and γ_7 is 80% conserved throughout the additional fifth exon, whereas the predicted four-exon γ_5 and γ_7 subunits differ greatly in sequence identities and length. The two large open triangles designate a pair of cysteine residues that are conserved amongst the putative VDCC γ subunits and may be involved in the formation of disulfide bridges. The transmembrane-spanning segments, as predicted by the TMpred program (Hofmann and Stoffel, 1993), are indicated by solid underlining. The residues highlighted in bold in the C-terminus of γ_7 identify the epitope for the anti-γ_7 antibody. (**B**) A schematic diagram of the γ_5 and γ_7 gene structure. The full-length genes are encoded by five exons interrupted by four introns, I1–I4. If the previously predicted four-exon γ_5 and γ_7 subunits were expressed, the extent of predicted read-through into intron 4 is displayed above the gene structure. The start codon, terminal amino acids of exon 4, and both normally spliced and intron-retained γ_5 or γ_7 are shown below the gene structure. (**C**) Hydropathy plots of the five-exon γ_5 and γ_7 subunits predicted by the TMpred program (Hofmann and Stoffel, 1993) compared with the previously predicted four-exon γ_5 and γ_7. Amino acid position is shown on the *x*-axis, and positive TMpred values indicate putative membrane-spanning regions. γ_7 and γ_5 are predicted to have four transmembrane-spanning α-helices with intracellular N- and C-termini.

but, even when extracellular $[Ba^{2+}]$ was increased to 10 mM, currents from GFP–Ca$_V$2.2/β_{1b}/α2δ_2/γ_7-transfected COS-7 cells remained extremely small (-0.23 ± 0.08 pA/pF at 0 mV, $n = 20$, $P <0.01$) (Figure 3A, lower trace, and B). In a recent report, it was stated that inhibition of Ca$_V$2.2 currents by the γ_2 subunit was dependent upon co-expression of an α2δ subunit (Kang *et al.*, 2001). To investigate if the same is

true of the much more robust suppressive effect of γ_7, recordings were made from cells in the absence of co-transfected α2δ_2 subunit. The histograms in Figure 3B show that the influence of the γ_7 subunit on Ca$_V$2.2/β_{1b} currents was independent of co-expression of an α2δ subunit (Ca$_V$2.2/β_{1b}, -14.9 ± 2.7 pA/pF at 0 mV in 1 mM Ba^{2+}, $n = 16$; Ca$_V$2.2/β_{1b}/γ_7, -0.02 ± 0.03 pA/pF at 0 mV in 10 mM Ba^{2+}; $n = 18$, $P <0.01$).
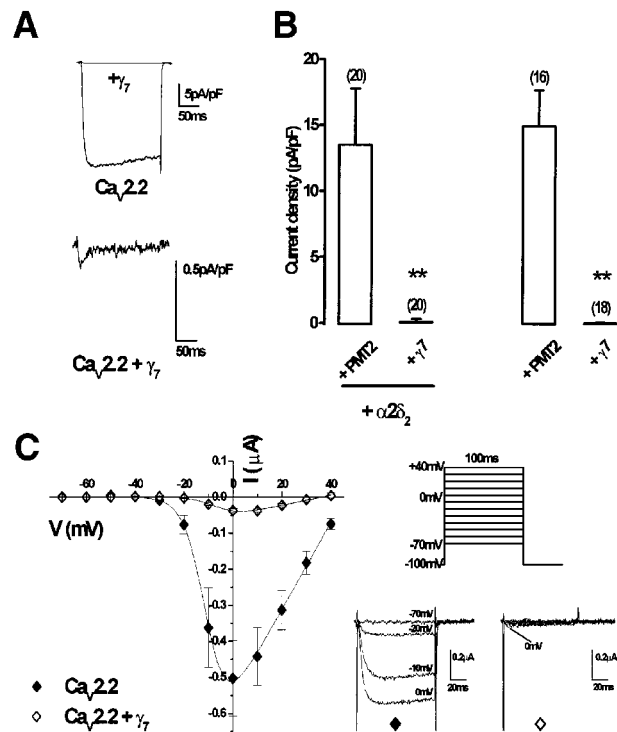
To examine whether these effects were peculiar to transfection in mammalian expression systems, we next looked at the effect of γ_7 on Ca_V2.2 currents expressed in *Xenopus* oocytes, where there cannot be any question as to whether all cDNAs are present in each cell. Figure 3C shows recordings made in 5 mM Ba^{2+} from *Xenopus* oocytes expressing Ca_V2.2/β_{1b} either with or without co-expression of γ_7. The maximum conductance (G_{max}), determined from the current–voltage (I–V) plots, was dramatically and significantly reduced when the human γ_7 subunit was co-expressed compared with oocytes where it was not, with a corresponding 92.6% reduction in peak current amplitude at 0 mV (Figure 3C and Table I). The half-maximal value for the voltage dependence of activation (V_{50}) was also shifted 3.4 mV more depolarized upon co-expression of γ_7. An almost identical 94% inhibition of Ca_V2.2/β_{1b}/$\alpha2\delta_2$ currents was observed by γ_7 in this system (data not shown). To examine whether the residual current represents the current induced by auxiliary subunits in *Xenopus* oocytes (Lacerda *et al.*, 1994), we examined currents from oocytes transfected with only the auxiliary subunit β_{1b}. However, we observed that these currents were also reduced from -28.1 ± 9.6 nA ($n = 10$) to -8.3 ± 5.3 nA ($n = 9$) upon co-expression of γ_7. We next investigated the effects of γ_7 on other Ca_Vα_1 subtypes. The γ_7 subunit also significantly reduced the G_{max} of Ca_V2.1/β_{1b} and Ca_V1.2/β_{1b} VDCCs by 48 and 52%, respectively

(Figure 4A and B, Table I). There were no significant effects of γ_7 on their voltage dependence of activation (Table I). Thus, the effect of γ_7 on these channels is not as striking as that seen with Ca_V2.2.

Together with the data generated in COS-7 cells, the near complete abolition of Ca_V2.2 current seen in *Xenopus*

Fig. 3. GFP–Ca_V2.2/β_{1b} cDNAs were transiently transfected into COS-7 cells with or without $\alpha2\delta_2$ and γ_7 subunits. (**A**) Example traces elicited by a 200 ms step depolarization to +10 mV from a holding potential of –80 mV in the presence of 1 mM Ba^{2+} (upper panel). In the presence of γ_7, extracellular Ba^{2+} solution was also increased to 10 mM (lower panel). (**B**) Histogram of mean current densities measured at +10 mV in 1 mM Ba^{2+} for controls and 10 mM Ba^{2+} in the presence of γ_7. Co-expression of γ_7 abolished currents in both the presence and absence of the $\alpha2\delta_2$ subunit. The number of experiments (n) for each condition is given in parentheses above the columns, and data from all cells tested are included (**$P <0.01$, Student's *t*-test). (**C**) Peak I–V relationships and individual representative traces for Ca_V2.2 (solid diamonds, $n = 26$) and Ca_V2.2 + γ_7 (open diamonds, $n = 24$), expressed in *Xenopus* oocytes with the β_{1b} auxiliary subunit were determined by measuring peak Ba^{2+} current amplitudes recorded during 100 ms test pulses between –70 and +40 mV (holding potential –100 mV; +10 mV increments; [Ba^{2+}] in extracellular medium: 5 mM).

Fig. 2. The expression profile of the human γ_7 subunit. (**A**) Multiple tissue northern blots probed specifically for the γ_7 subunit show two mRNA species of ~2.4 and 3.0 kb that are localized specifically to human brain. Multiple brain region blots (**B** and **C**) show that the γ_7 subunit is expressed in all the individual brain regions probed. The bottom section of each panel displays the mRNA detected by the control β-actin probe for each blot.

Table I. Influence of the γ_7 subunit on the activation properties of VDCCs expressed in *Xenopus* oocytes

Channel	Activation				n
	V_{50} (mV)	k	G_{max} (μS)	Peak I_{Ba} (μA)	
Ca_V2.2	-7.34 ± 0.79	4.34 ± 0.24	12.7 ± 2.29	-0.50 ± 0.10	26
Ca_V2.2 + γ_7	-3.88 ± 0.92**	4.66 ± 0.40	1.50 ± 0.27***	-0.04 ± 0.01***	24
Ca_V2.1	-0.63 ± 0.73	5.03 ± 0.24	5.76 ± 0.95	-0.17 ± 0.02	17
Ca_V2.1 + γ_7	0.92 ± 0.68	4.71 ± 0.41	2.98 ± 0.46**	-0.09 ± 0.02**	19
Ca_V1.2	-0.68 ± 2.08	6.80 ± 0.31	5.88 ± 1.40	-0.17 ± 0.04	10
Ca_V1.2 + γ_7	1.75 ± 0.70	5.68 ± 0.59	2.84 ± 0.57*	-0.10 ± 0.02	14

Data are expressed as mean $\pm$ SEM of the number of replicates, n. *$P <0.05$, **$P <0.01$ and ***$P <0.001$ according to an unpaired Student's *t*-test. The peak I_{Ba} was at +10 mV for Ca_V2.1 and Ca_V1.2 and at 0 mV for Ca_V2.2.
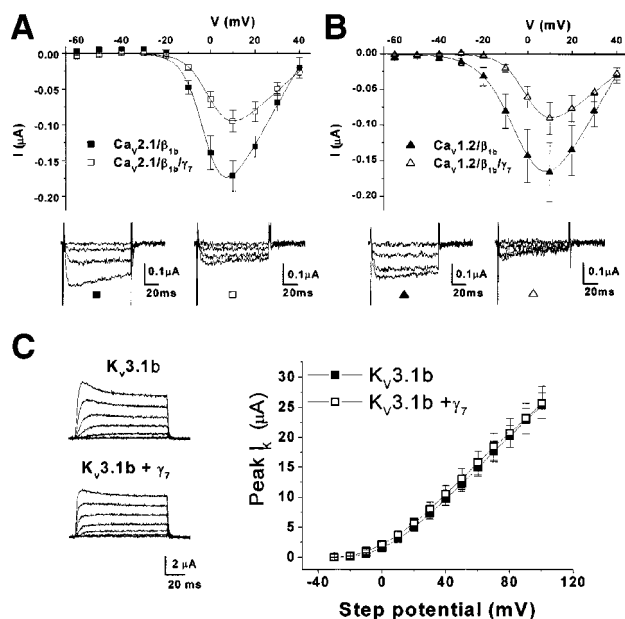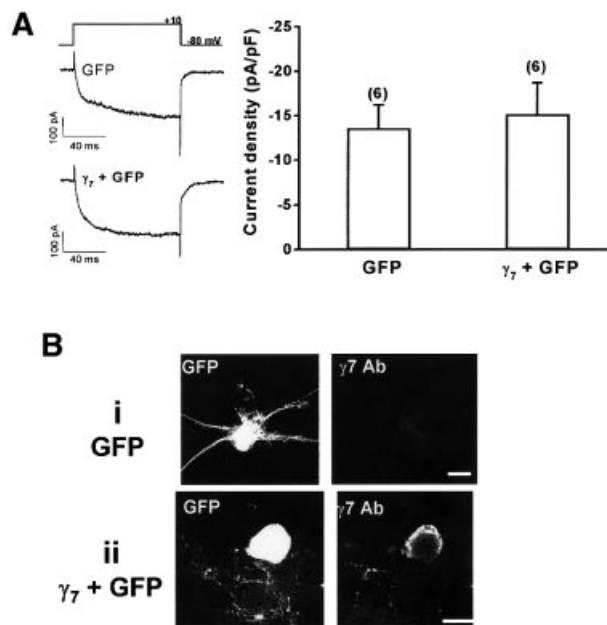
Fig. 4. Effect of heterologous expression of γ_7 with other channels. (**A** and **B**) Mean I–V relationships and individual representative traces for (A) $Ca_V2.1$ (solid squares, $n = 17$) and $Ca_V2.1 + \gamma_7$ (open squares, $n = 19$); (B) $Ca_V1.2$ (solid triangles, $n = 10$) and $Ca_V1.2 + \gamma_7$ (open triangles, $n = 15$), expressed in *Xenopus* oocytes with β_{1b}. Peak Ba^{2+} current amplitudes were recorded during 100 ms test pulses between –70 and +40 mV (holding potential –100 mV; +10 mV increments; $[Ba^{2+}]$ 10 mM). (**C**) Peak I–V relationship for $K_V3.1b$ (solid squares, $n = 10$), and $K_V3.1 + \gamma_7$ (open squares, $n = 10$), and current traces for $K_V3.1$ (top left panel) and $K_V3.1 + \gamma_7$ (bottom left panel) expressed in *Xenopus* oocytes. Holding potential was –100 mV, and steps were between –30 and +100 mV for 100 ms. The scale bar refers to both panels.

Fig. 5. Effect of heterologous expression of γ_7 in cultured sympathetic neurones. (**A**) Left: example traces from sympathetic neurones transiently transfected with GFP or GFP and the γ_7 subunit, elicited by a 100 ms step depolarization to +10 mV from a holding potential of –80 mV in medium containing 10 mM Ba^{2+}. Right: histogram of mean current densities measured from sympathetic neurones at +10 mV. The number of experiments (n) for each condition is given in parentheses above the columns. (**B**) Upper row: a GFP-transfected sympathetic neurone (left panel), showing lack of immunostaining for endogenous γ_7 (right panel). Lower row: a GFP- plus γ_7-transfected sympathetic neurone (left panel), showing immunostaining for γ_7 (middle panel). Data are representative of three transfections. Scale bars = 15 µm.

oocytes upon co-expression of the γ_7 subunit suggests that it may be affecting the expression of these channels rather than altering their biophysical properties. However, since the effect of γ_7 on the Ba^{2+} currents through $Ca_V2.2$ VDCCs expressed in COS-7 cells or *Xenopus* oocytes was so striking, we investigated the possibility that it downregulates other heterologously expressed ion channels by co-expressing it with the Shaw-like voltage-dependent potassium channel, $K_V3.1b$. Figure 4C shows representative traces and the peak I–V relationship of $K_V3.1b$ currents expressed in *Xenopus* oocytes alone and co-expressed with the γ_7 subunit, which indicate that the γ_7 subunit had no effect on the peak current amplitude of heterologously expressed $K_V3.1b$ channels.

Influence of the γ_7 subunit on endogenous Ca^{2+} currents recorded from cultured sympathetic neurones

We investigated the electrophysiological consequence of the acute expression of γ_7 upon the endogenous VDCC currents from sympathetic neurones of the rat superior cervical ganglion (SCG). These neurones express 80–90% N-type and 10% L-type current (Plummer *et al.*, 1989; Delmas *et al.*, 1998) and provided a vehicle in which we could determine if the γ_7 subunit could exert its influence upon pre-existing Ca^{2+} channels. Whole-cell patch-clamp recordings, performed 36–48 h post-isolation and transfection from control sympathetic neurones transfected with

the GFP marker, gave a mean I_{Ba} current density at 0 mV of –13.6 ± 2.6 pA/pF ($n = 6$). However, this was not significantly altered in neurones transfected with GFP and the γ_7 subunit (–15.2 ± 3.5 pA/pF, $n = 6$) (Figure 5A). Expression of γ_7 protein in γ_7-transfected neurones was verified by immunocytochemistry (Figure 5B), which also demonstrated the presence of only a very low level of immunoreactivity for endogenous γ_7 in neurones transfected with GFP alone (Figure 5B). Although the morphology of sympathetic neurones cultured for 36–48 h is quite variable, in a preliminary observation, we also noted an alteration in neurite morphology in sympathetic neurones transfected with γ_7 (Figure 5B), but this will require further detailed examination in a future study. It would therefore appear that the γ_7 subunit is unable to acutely influence the properties of pre-existing N-type VDCCs in these neurones, and that γ_7 does not co-exist endogenously in SCG neurones with N-type channels.

Immunocytochemical analysis of the effects of the γ_7 subunit

The subcellular distribution of the expressed γ_7 subunit and its effects upon the expression of $Ca_V2.2$ subunits were determined using immunocytochemistry and confocal laser scanning microscopy. When the γ_7 subunit alone was transiently transfected into COS-7 cells (Figure 6A), expression of γ_7 protein was observed throughout the cytoplasm and not specifically associated with the plasma membrane (delineated by Oregon Green–phalloidin). Figure 6B shows the typical fluores-
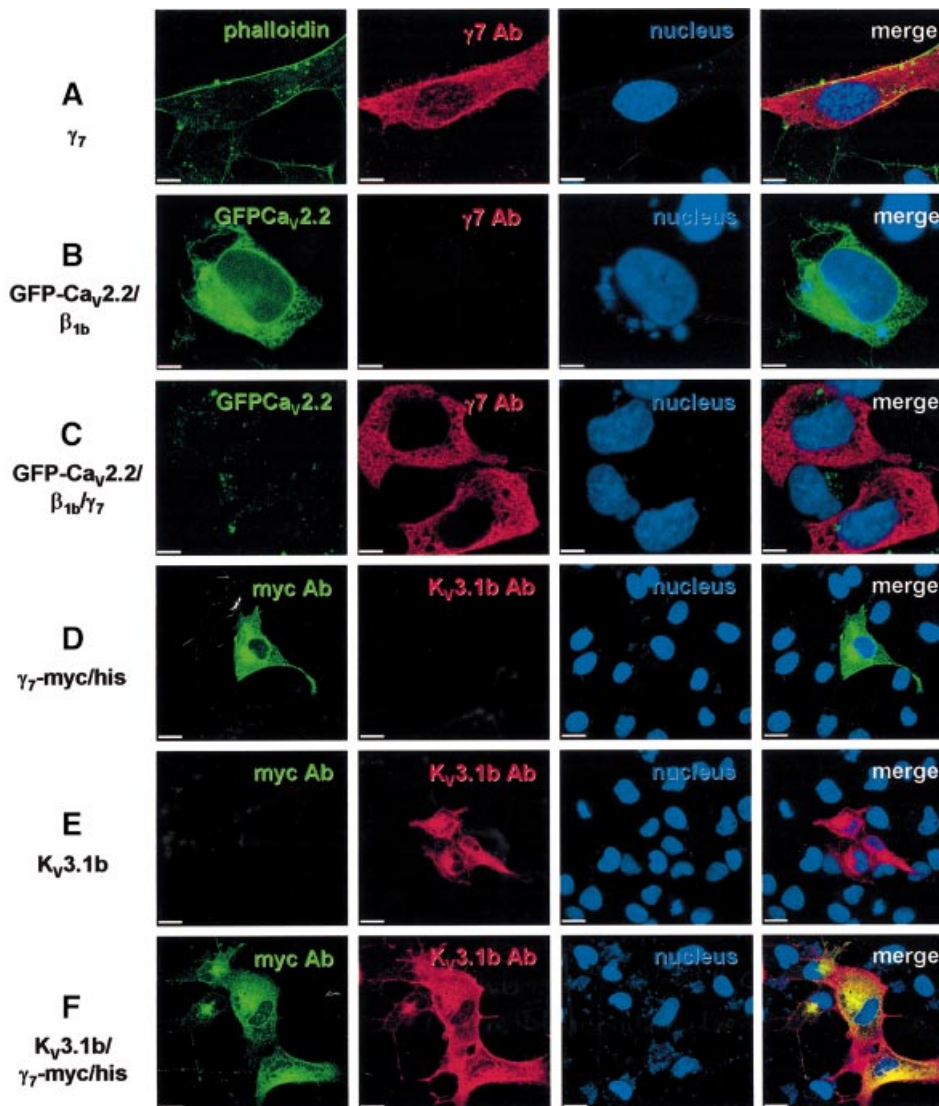
Fig. 6. Co-expression of γ7 with GFP–CaV2.2 almost abolishes GFP fluorescence in COS-7 cells. Cells were transfected with (**A**) the γ7 subunit alone, (**B**) GFP–CaV2.2/β1b, (**C**) GFP–CaV2.2/β1b/γ7, (**D**) γ7-myc/his, (**E**) KV3.1b or (**F**) KV3.1b/γ7-myc/his. The panels in column 1 show staining with Oregon Green–phalloidin, GFP fluorescence or FITC-labelled myc Ab as stated; the panels in column 2 show Texas red staining for the γ7 subunit or KV3.1b subunit as stated; the panels in column 3 display the blue DAPI staining of the nucleus; and the panels in column 4 show the merged images. The scale bar in (A–C) represents 10 μm and in (D–F), 20 μm.

cence pattern of a cell transiently transfected with GFP–CaV2.2/β1b. Figure 6C shows two cells where the γ7 subunit has also been co-transfected. A striking reduction in the fluorescence of GFP–CaV2.2 was observed upon co-expression of the γ7 subunit, whilst the γ7 levels remained comparable with those in cells transfected with the γ7 subunit alone.

Immunocytochemical methods also confirmed the earlier electrophysiological findings that the γ7 subunit does not adversely affect the expression of the KV3.1b subunit. Figure 6D displays the expression of a γ7-myc/his fusion protein expressed alone in a COS-7 cell. The expression pattern of this construct is similar to that of the untagged γ7 (Figure 6A). Shown in Figure 6E is the expression of KV3.1b when transfected alone. The distribution and the expression level of KV3.1b were unaltered by the co-expression of the γ7-myc/his fusion protein (Figure 6F).

In transient transfections, co-transfected subunits are not always co-expressed in every cell. We therefore sought to quantify the extent of the reduction in observed GFP–CaV2.2 fluorescence caused by γ7 subunit co-expression. This was measured by counting the number of GFP-positive cells in both the GFP–CaV2.2/β1b- and GFP–CaV2.2/β1b/γ7-transfected cultures. The mean percentage of the total cells per 16 mm^2 field of view with GFP–CaV2.2 fluorescence, which entirely co-localizes with β1b expression, was reduced from $16.4 \pm 3.4\%$ in GFP–CaV2.2/β1b-transfected cells to $3.3 \pm 0.7\%$ in cells additionally transfected with the γ7 subunit (Figure 7A). The same histogram also shows that almost all cells that exhibited GFP–CaV2.2 fluorescence in the CaV2.2/β1b/γ7 transfections were also labelled for γ7 ($3.0 \pm 0.7\%$), implying that there is some residual GFP–CaV2.2 fluorescence in some cells expressing the γ7 subunit. The
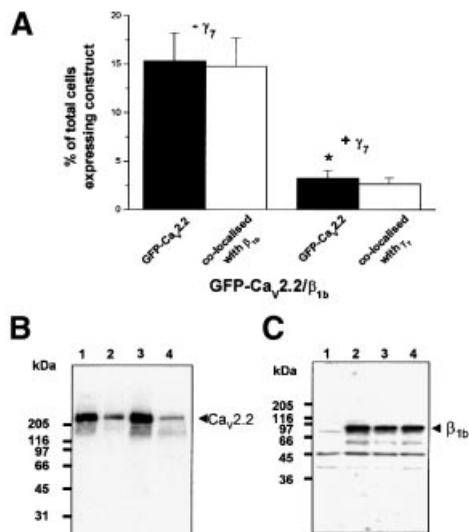
Fig. 7. The effect of co-expression of γ_7 subunit on the expression of Ca$_V$2.2 in COS-7 cells. (**A**) Histogram of the mean percentage of total cells per field of view (±SEM) expressing GFP–Ca$_V$2.2 and those which are co-localized with β_{1b} or γ_7 (visualized with Texas red), following transfection with the subunit combinations stated. (**B**) Western blotting and immunodetection using anti-rabbit brain Ca$_V$2.2 II–III loop Ab. Lane 1, GFP–Ca$_V$2.2; lane 2, GFP–Ca$_V$2.2 and γ_7; lane 3, Ca$_V$2.2 Δ3′UTR; lane 4, Ca$_V$2.2 Δ3′UTR and γ_7. The positions of molecular weight markers are shown on the left. Blots are representative of three similar experiments. (**C**) Western blotting and immunodetection with anti-β_{1b} Ab. Lane 1, untransfected COS-7 cells; lane 2, GFP–Ca$_V$2.2/β_{1b}; lane 3, GFP–Ca$_V$2.2/β_{1b}/γ_7; lane 4, GFP–Ca$_V$2.2/β_{1b}/γ_7-myc/his.

specificity of the γ_7 antibody (Ab) was determined by western blotting where it was observed to label a major band at ~35 kDa when γ_7 was expressed in COS-7 cells (data not shown).

Effect of co-expression of the γ_7 subunit on the Ca$_V$2.2 protein levels

GFP–Ca$_V$2.2 or untagged Ca$_V$2.2 expressed in COS-7 cells are detectable by western blot using an Ab against the II–III loop of Ca$_V$2.2 (band at ~240 kDa). When the γ_7 subunit was co-expressed with either the GFP–Ca$_V$2.2 or untagged Ca$_V$2.2, the intensity of the Ca$_V$2.2 band was greatly reduced, but expression of the protein was not completely abolished (Figure 7B). No smaller molecular weight bands were observed that might represent degradation products of the GFP–Ca$_V$2.2 or untagged Ca$_V$2.2 or partially synthesized protein. Similar results were obtained both in the absence and presence of the auxiliary β_{1b} subunit, and also using the anti-GFP Ab (data not shown). Additionally, the co-expression of γ_7 or γ_7-myc/his with Ca$_V$2.2/β_{1b} did not reduce the expression of the β_{1b} subunit (Figure 7C). These data extend the findings from confocal imaging and electrophysiology experiments by revealing that the γ_7 subunit suppresses the expression of GFP–Ca$_V$2.2 protein rather than interfering with the correct conformational folding or trafficking of the GFP-labelled protein that could result in reduced fluorescence or recorded current densities.

Discussion

We have described the identification of two genes that encode putative VDCC subunits γ_7 and γ_5, by their

sequence and structural homology to the mouse *stargazin* gene (*cacng2*), and have cloned and expressed the cDNA for both human and mouse γ_7. The γ_7 subunit is predicted to be a 275 amino acid, 31 kDa protein possessing four transmembrane-spanning domains with intracellular N- and C-termini. The *in silico* sequence for γ_5 also predicts a 275 amino acid, 31 kDa protein with identical transmembrane topology to γ_7. Their overall size is much closer to that predicted for the skeletal muscle γ_1 subunit than for the neuronal γ_2, γ_3 and γ_4 subunits. Their sequence homology with the γ_1 subunit is extremely low, but both the γ_7 and γ_5 subunits possess ~25% identity to the human γ_2 subunit, with higher degrees of conservation occurring in the predicted transmembrane regions (up to 36%). It must also be noted that the C-termini of the γ_7 and γ_5 subunits differ from those of γ_2, γ_3 and γ_4 subunits, as they are much shorter and lack the classical consensus motif for interaction with PDZ domains (Kornau *et al.*, 1997; Tomita *et al.*, 2001). This C-terminal motif of γ_2 (also present in γ_3 and γ_4 subunits) has been shown to play a crucial role in trafficking AMPA (α-amino-3-hydroxyl-5-methyl-4-isoxazolepropionate) receptor subunits to their correct location in the postsynaptic density (Chen *et al.*, 2000). This difference suggests that γ_7 and γ_5 may have a different function from that of the γ_2, γ_3 and γ_4 subunits.

The γ_7 and γ_5 subunits are, however, 70.5% identical to one another and, unlike all other putative γ subunits, are assembled from five exons, the first four of which are identical to exons 1–4 of the genes encoding the previously predicted γ_7 and γ_5 subunits (Burgess *et al.*, 1999, 2001). Sequence analysis of the BAC clones in which these genes were found suggests that the previously predicted four-exon γ_7 and γ_5 subunit sequences result from inclusion of intronic sequences at the exon 4–intron 4 boundary of *CACNG7* and *CACNG5* (Figure 1B). Inspection of the sequence of intron 4 of *CACNG7* and *CACNG5* reveals that in-frame stop codons are found 25 and 319 nucleotides, respectively, downstream of the exon 4–intron 4 boundary. The final eight C-terminal amino acids of the predicted four-exon γ_7 are encoded by the first 24 bases of intron 4 before a stop codon. Similarly, the C-terminal 106 amino acids of the predicted four-exon γ_5 would be encoded by the entirety of intron 4, resulting in a C-terminal γ_5 sequence which has extremely low sequence homology to the other γ subunits.

The sequence of the corresponding mouse orthologues of the predicted human four-exon γ_7 and γ_5 can be deduced by analysis of the relevant mouse BACs. However, the stop codons within the fourth intron of each mouse gene are not in the same or even similar positions to their human equivalents, and their C-terminal regions do not retain homology to their human counterparts. In contrast, the *in silico* prediction of the mouse five-exon γ_5 sequence exhibits 89.5% identity to that of human γ_5 at the nucleic acid level and 97% identity at the protein level. Our results strongly indicate that the previously predicted four-exon γ_5 and γ_7 subunits are not expressed *in vivo*.

The γ_5 and γ_7 subunits represent a distinct subdivision of the γ subunit family of proteins identified by structural and sequence homology to stargazin. In addition to the lower sequence homology to the neuronal γ_2, γ_3 and γ_4 subunits, the identification of these gene products, assembled from five exons rather than four, as in the case for the *stargazin*

gene and its closer homologues, is evidence for further evolutionary diversion from a common ancestor. This conclusion was also reached in a recent genomic analysis of the γ subunit superfamily (Chu *et al.*, 2001).

Northern blot analysis of the γ₇ mRNA revealed it to be expressed exclusively in neuronal tissue. Two probes were used in different hybridizations, one specific for full-length γ₇ and the other, used in RT–PCR-based expression analysis in the previous study (Burgess *et al.*, 2001), which would detect mRNAs for both full-length γ₇ and the putative four-exon γ₇. Both probes hybridized to ~2.4 and ~3 kb mRNAs, with identical expression patterns in all tissues in which they are expressed. Thus the two bands cannot represent separate transcripts for the previously predicted four-exon γ₇ and the five-exon γ₇ described here. It would appear highly unlikely, given these data, that the four-exon γ₇ is expressed *in vivo*.

Co-expression of the γ₇ subunit almost completely abolished Ba^{2+} current through N-type Ca$_V$2.2 VDCCs expressed in both *Xenopus* oocyte and COS-7 mammalian expression systems. It also significantly reduced maximum Ba^{2+} conductance in the non-N type Ca$_V$2.1 and Ca$_V$1.2 VDCCs, but the effects were not so pronounced. In contrast to the effects of the neuronal γ₂ subunit, which has been reported in a previous study to inhibit N-type Ca$_V$2.2/β₃/α2δ₁ currents by ~37% (Kang *et al.*, 2001), the influence of the γ₇ subunit is not dependent upon co-expression of an exogenous α2δ subunit as part of the Ca^{2+} channel complex.

Several mechanisms could underlie the suppression of VDCC currents by the γ₇ subunit, including: (i) interference with the functioning of the channel at the plasma membrane; (ii) inhibition of the delivery of the channel to the plasma membrane; (iii) prevention of the correct folding of the pore-forming subunit; (iv) more rapid protein degradation; and (v) suppression of channel protein synthesis.

Confocal imaging of COS-7 cells transiently expressing N-terminally tagged GFP–Ca$_V$2.2 Ca^{2+} channel complexes revealed that co-expression of the γ₇ protein, which itself is highly expressed throughout the cell, resulted in an almost complete loss of GFP fluorescence. This suggested reduced synthesis or stability of GFP–Ca$_V$2.2, or interference of the γ₇ subunit with the correct folding of the GFP-tagged protein. Western blot analysis of the levels of both GFP–Ca$_V$2.2 and untagged Ca$_V$2.2 revealed that co-expression of γ₇ results in a much reduced steady-state level of Ca$_V$2.2. This is likely to be due to a reduction in the level of Ca$_V$2.2 protein synthesized when γ₇ is co-expressed, because no smaller molecular weight products of degradation were evident. It nevertheless is also possible that γ₇ induces rapid and complete targeting of Ca$_V$2.2 to a degradation pathway. Whilst northern blot analysis is required to examine whether the Ca$_V$2.2 mRNA level is reduced in the presence of γ₇, we have noted in the present study that the reduction in Ca$_V$2.2 protein level still occurs following the removal of its 3′-untranslated region (UTR) (Figure 7B), which has been implicated in message stability (Schorge *et al.*, 1999).

These results raised the possibility that the γ₇ was causing a non-specific inhibition of transcription or translation. However, we have shown that the influence of γ₇ does not cause a generalized down-regulation of all heterologously expressed ion channels, because the I–V relationship for the voltage-dependent potassium channel K$_V$3.1b expressed in *Xenopus* oocytes was unaffected by co-expression of the γ₇ subunit. Furthermore, immuno-cytochemistry experiments confirmed that the expression of K$_V$3.1b in COS-7 cells was unaltered by the co-expression of the γ₇ subunit and there was little effect on expression of the VDCC β₁$_b$ subunit.

Our results bear a striking resemblance to the dominant-negative synthesis suppression of the Ca$_V$2.2 subunit induced by the co-expression of truncated Ca$_V$2.2 constructs (Raghib *et al.*, 2001). In that investigation, it was proposed that the translation of full-length Ca$_V$2.2 was halted when domain I or domain I–II of Ca$_V$2.2 interacted with the initially synthesized transmembrane α-helices of the nascent full-length Ca$_V$2.2. We do not yet know if a similar mechanism might be invoked for the down-regulation of Ca$_V$2.2 by γ₇.

Further evidence indicates that the influence of γ₇ expression may be upon newly synthesized Ca$_V$2.2 protein. Transient expression of the γ₇ subunit in sympathetic neurones did not significantly alter endogenous (largely N-type) calcium current densities. The γ₇ subunit therefore does not affect the function of pre-existing functional N-type channels.

It appears that the influence of γ₇ on VDCC expression and function is via a mechanism unlike that reported previously for the other stargazin-like proteins. Nevertheless, in the present study, inhibition of expression by the γ₇ subunit is apparently specific for VDCC subunits, particularly Ca$_V$2.2, because its co-expression with K$_V$3.1b did not inhibit the expression of the potassium channel.

That γ₇ is actually a subunit of a functional plasma membrane calcium channel complex appears unlikely, at least for Ca$_V$2.2. This is reinforced by the absence of significant endogenous γ₇ in sympathetic neurones, where the current is predominantly N-type. Future work will examine in which cell types γ₇ is expressed endogenously in the brain, and whether its endogenous function is to down-regulate Ca$_V$2.2 expression.

Materials and methods

Text-based in silico cloning

The GenBank and EMBL databases were searched for sequences possessing homology to the full-length sequence of the mouse *stargazin* gene (Letts *et al.*, 1998). ESTs and genomic sequences from both databases were clustered to identify overlapping identical sequence belonging to the same transcript using the GCG package (Wisconsin Package Version 9.0, Genetics Computer Group) and a program developed by GlaxoSmithKline Research and Development Bioinformatics group, termed ESTBlast (Gill *et al.*, 1997). Multiple sequence alignments of conceptually translated proteins were aligned using the Clustal_W algorithm (Omiga 1.1, Oxford Molecular Group, Oxford, UK).

Cloning of stargazin-like genes

An RT–PCR approach was used to amplify the complete ORFs or partial sequences of predicted γ-subunits either from cDNA derived from RNA or from overlapping partial clones. Human brain total RNA (Invitrogen, Paisley, UK) or mouse cerebellar total RNA purified from the cerebella of 31-day-old mice using the RNeasy kit (Qiagen, Crawley, UK) were used to generate cDNA using the Superscript Pre-amplification System (Invitrogen) primed with random hexamers.

Cloning human γ_7. The γ_7, 487 bp fragment predicted by *in silico* cloning was amplified from 25 ng of Superscript-synthesized human brain cDNA using 25 pmol each of primer pair 5′-CGGGAGAAAGG-TCGCTGT-3′ and 5′-TCATTTGGATGGACACGTCG-3′. This was then extended by 5′ and 3′ RACE protocols using Marathon Ready total human brain cDNA (BD Biosciences Clontech, Basingstoke, UK). The complete nucleotide sequence of γ_7 was assembled from two of the generated RACE clones and the original 487 bp clone by a splice overlap PCR protocol using a primer pair specific for the predicted ORF. The cDNA was sequenced then subcloned into a modified pMT2 expression vector (Swick *et al.*, 1992). Human γ_7-myc/his was constructed by amplifying the complete ORF minus the stop codon from the pMT2-γ_7 clone and inserting the fragment in-frame into the multiple cloning site of pCDNA3.1 myc/his A (+) (Invitrogen) using the *Not*I and *Apa*I restriction sites.

Cloning mouse γ_7. The nucleotide sequence of the human γ_7 was compared with the HTGS subset of GenBank using BLASTn and tBLASTn with default parameters. The complete coding sequence was found within chromosome 19 BAC AC079557 and used to design gene-specific primers 5′-ATGAGTCACTGCAGCAGCCG-3′ and 5′-TCA-GCACGGCGAAGTGGAGA-3′. The complete ORF was amplified in a single PCR from 20 ng of mouse cerebellar cDNA and cloned into pCR4-TOPO for sequencing, and subcloned into pMT2 and pRK5 for expression in *Xenopus* oocytes/COS-7 cells or SCG neurones, respectively.

Northern blots
Human 12-lane multiple tissue blots and brain II and IV blots (BD Biosciences Clontech) were hybridized at 65°C in ExpressHyb solution (BD Biosciences Clontech) according to the manufacturer's instructions. The α-^{32}P-radiolabelled γ_7 probes corresponding to nucleotides 576–763 or 80–482 were assembled according to the Strip-EZ DNA Probe Synthesis Removal Kit [Ambion (Europe) Ltd, Huntingdon, UK]. The final stringency wash performed was $0.1\times$ SSC, 0.1% SDS at 65°C.

Other cDNA clones
The following cDNAs were used: rabbit $Ca_V2.2$ (D14157), N-terminal GFP-tagged rabbit $Ca_V2.2$ (Raghib *et al.*, 2001), rabbit $Ca_V2.2$ $\Delta3'UTR$, rabbit $Ca_V2.1$ (X57689), rat brain $Ca_V1.2$ (isoform CII, M67515), rat β_{1b} (X61394, except R417S, V435, V449A, W492R, V511A, a gift from Dr T.P.Snutch), mouse $\alpha2\delta_2$ (AF247139, common brain splice variant), mut-3b GFP (M62653, except S72A and S65G, a gift from Dr T.E.Hughes) and rat $K_V3.1b$ (M68880). The 3′-UTR of rabbit $Ca_V2.2$ was removed to generate $Ca_V2.2$ $\Delta3'UTR$, by introducing an *Spe*I site immediately after the stop codon by PCR and subcloning the $Ca_V2.2$ back into the vector. All cDNAs were subcloned into expression vector pMT2 (Swick *et al.*, 1992), with the exception of $K_V3.1b$ that was in pRC-CMV.

Cell culture and transfections
Monkey COS-7 cells were cultured as previously described (Brice *et al.*, 1997). Transfection was performed with Geneporter transfection reagent (Gene Therapy Systems, San Diego, CA). Cells were plated onto coverslips 2–3 h prior to transfection. The DNA and Geneporter reagent (2 µg and 10 µl, respectively) were each diluted in 500 µl of serum-free medium, mixed, and applied to the cells. The α_1, β, $\alpha2\delta$ and γ subunits were mixed and transfected in a 1:1:1:1 ratio by DNA weight. In the absence of $\alpha2\delta$ and/or γ_7 subunit, blank pMT2 vector was substituted. After 3.5 h, 1 ml of medium containing 20% serum was added to the cells, which were then incubated at 37°C for 3 days. Prior to electro-physiological recording, cells were re-plated using a non-enzymatic cell dissociation solution (Sigma, Dorset, UK) and maintained at 27°C for between 2 and 6 h. Cells for immunocytochemistry were not re-plated.

Electrophysiology
Xenopus oocytes. Xenopus oocytes were prepared, injected and utilized for electrophysiology as previously described (Canti *et al.*, 1999), with the following exceptions. Plasmid cDNAs for the different VDCC subunits were mixed in a weight ratio of 1:1:1:1. The recording solution for $Ca_V2.2$-injected oocytes contained: 5 mM $Ba(OH)_2$, 80 mM TEA-OH, 2 mM CsOH and 5 mM HEPES (pH 7.4 with methanesulfonic acid). The $Ba(OH)_2$ concentration was raised to 10 mM for recording $Ca_V1.2$ and $Ca_V2.1$ currents. $K_V3.1b$ currents were recorded 3 days after intranuclear injection of oocytes with 9 nl of cDNA together with an equal amount of γ_7 in pMT2, or water for the control. The external medium contained: 96 mM NaCl, 5 mM HEPES, 2 mM KCl, 1 mM $MgCl_2$ and 1.8 mM $CaCl_2$ (pH 7.4).

COS-7 cells. Recordings were made from fluorescent COS-7 cells expressing GFP–$Ca_V2.2$. Because GFP–$Ca_V2.2$ was only weakly fluorescent, free GFP (ratio 0.1) was included in the transfection to identify transfected cells from which recordings were made. Whole-cell patch–clamp recording was performed as previously described (Meir *et al.*, 2000). Ba^{2+} (1 mM) was used as a charge carrier, except in the presence of γ_7 subunit where 10 mM Ba^{2+} was also used. Experiments were performed at room temperature. Data are expressed as mean $\pm$ SEM. Statistical analysis was performed using paired or unpaired Student's *t*-test, as appropriate.

SCG preparation, transfection and electrophysiology
Sympathetic neurones were isolated from 17-day-old Sprague–Dawley rats killed by CO_2 inhalation, following a modified procedure described by Delmas *et al.* (1998), in which collagenase type IA (500 U/ml, Sigma) and trypsin type XI (3000 U/ml, Sigma) were used. Aliquots of the cell suspension were transferred immediately to the electroporation cuvettes together with 10 µg of each of the cDNAs to be transfected. After electroporation (Morales *et al.*, 2000) (250 V, 900 µF, EasyjecT Plus, EquiBio, Ashford, UK), the cells were resuspended in pre-warmed growth medium, plated on poly-L-lysine (Sigma)-coated Petri dishes and incubated at 37°C, 5% CO_2, for 36–48 h before use for immunocyto-chemistry or electrophysiological experiments. Currents were elicited in the whole-cell patch–clamp configuration from a holding potential of –80 mV by 100 ms steps from –40 to +40 mV. Otherwise all other recording conditions were as described above, with the exception of the addition of 0.5 µM tetrodotoxin to the extracellular solution.

Antibody generation
The peptide identified in Figure 1A was synthesized by standard solid-phase techniques, purified by gel filtration chromatography and used to generate polyclonal anti-γ_7 rabbit Abs as previously described (Amaya *et al.*, 2000). His-tagged rat β_{1b} subunit, purified essentially as previously described (Canti *et al.*, 2001), was used to generate the polyclonal rabbit β_{1b} Ab.

Immunocytochemistry
COS-7 cells or SCG neurones were fixed and permeabilized for immunocytochemistry essentially as previously described (Brice *et al.*, 1997). Primary Abs, affinity-purified anti- γ_7, anti-myc (Autogen-Bioclear, Calne, UK) and anti-$K_V3.1b$ (Alomone labs, Jerusalem, Israel) were used at 0.8, 4 and 1.5 µg/ml, respectively. Anti-β_{1b} antiserum was used at 1:1000 dilution. Secondary biotin-conjugated goat anti-mouse (Molecular Probes, Eugene, OR) or goat anti-rabbit (Sigma, Dorset, UK) Abs were applied at 10 and 5 µg/ml, respectively. Texas red- or fluorescein isothiocyanate (FITC)-conjugated streptavidin were applied at 3.33 µg/ml. In co-labelling experiments, $K_V3.1b$ was labelled with goat anti-rabbit Texas red-conjugated secondary Ab at 10 µg/ml (Molecular Probes). In some experiments, cells were incubated for 20 min with Oregon Green–phalloidin (6.6 µM, Molecular Probes). The nuclear dye 4′,6-diamidino-2-phenylindole (DAPI; 300 nM, Molecular Probes) was also used to visualize the nucleus. Cells were examined on a con-focal scanning laser microscope (Leica TCS SP, Milton Keynes, UK). All images were scanned sequentially to eliminate cross-talk, and photomultiplier settings were kept constant in each experiment.

Western blotting
COS-7 cells were processed as previously described (Raghib *et al.*, 2001). Samples (50 µg of total protein/lane in Figure 7B and 10 µg of total protein/lane in Figure 7C) were separated by SDS–PAGE using 4–20% gradient gels and then transferred electrophoretically to polyvinylidene fluoride membranes. The membranes were blocked with 3% bovine serum albumin (BSA) for 5 h at 55°C and then incubated overnight at 20°C with either 1.2 µg/ml of an anti-peptide Ab raised in rabbits against residues 846–861 within the II–III loop of rabbit brain $Ca_V2.2$ (Raghib *et al.*, 2001), or a 1:1000 dilution of anti-rat β_{1b} antiserum. Secondary Ab (a 1:1000 dilution of goat anti-rabbit IgG–horseradish peroxidase conjugate) was added and the membranes incubated for 1 h. Following extensive washing, bound Abs were detected using enhanced chemiluminescence (ECL, Amersham Pharmacia Biotech, Little Chalfont, UK).

References

Ahern,C.A. *et al.* (2001) Modulation of L-type Ca²⁺ current but not activation of Ca²⁺ release by the γ₁ subunit of the dihydropyridine receptor of skeletal muscle. *BMC Physiol.*, **1**, 8.

Amaya,F., Decosterd,I., Samad,T.A., Plumpton,C., Tate,S., Mannion,R.J., Costigan,M. and Woolf,C.J. (2000) Diversity of expression of the sensory neuron-specific TTX-resistant voltage-gated sodium ion channels SNS and SNS2. *Mol. Cell. Neurosci.*, **15**, 331–342.

Birnbaumer,L., Qin,N., Olcese,R., Tareilus,E., Platano,D., Costantin,J. and Stefani,E. (1998) Structures and functions of calcium channel β subunits. *J. Bioenerg. Biomembr.*, **30**, 357–375.

Black,J.L.,III and Lennon,V.A. (1999) Identification and cloning of putative human neuronal voltage-gated calcium channel γ-2 and γ-3 subunits: neurologic implications. *Mayo Clin. Proc.*, **74**, 357–361.

Brice,N.L., Berrow,N.S., Campbell,V., Page,K.M., Brickley,K., Tedder,I. and Dolphin,A.C. (1997) Importance of the different β subunits in the membrane expression of the α1A and α2 calcium channel subunits: studies using a depolarization-sensitive α1A antibody. *Eur. J. Neurosci.*, **9**, 749–759.

Burge,C. and Karlin,S. (1997) Prediction of complete gene structures in human genomic DNA. *J. Mol. Biol.*, **268**, 78–94.

Burgess,D.L., Davis,C.F., Gefrides,L.A. and Noebels,J.L. (1999) Identification of three novel Ca²⁺ channel γ subunit genes reveals molecular diversification by tandem and chromosome duplication. *Genome Res.*, **9**, 1204–1213.

Burgess,D.L., Gefrides,L.A., Foreman,P.J. and Noebels,J.L. (2001) A cluster of three novel Ca²⁺ channel γ subunit genes on chromosome 19q13.4: evolution and expression profile of the γ subunit gene family. *Genomics*, **71**, 339–350.

Canti,C., Page,K.M., Stephens,G.J. and Dolphin,A.C. (1999) Identification of residues in the N terminus of α1B critical for inhibition of the voltage-dependent calcium channel by Gβγ. *J. Neurosci.*, **19**, 6855–6864.

Canti,C., Davies,A., Berrow,N.S., Butcher,A.J., Page,K.M. and Dolphin,A.C. (2001) Evidence for two concentration-dependent processes for β-subunit effects on α1B calcium channels. *Biophys. J.*, **81**, 1439–1451.

Catterall,W.A. (2000) Structure and regulation of voltage-gated Ca²⁺ channels. *Annu. Rev. Cell. Dev. Biol.*, **16**, 521–555.

Chen,L., Chetkovich,D.M., Petralia,R.S., Sweeney,N.T., Kawasaki,Y., Wenthold,R.J., Bredt,D.S. and Nicoll,R.A. (2000) Stargazin regulates synaptic targeting of AMPA receptors by two distinct mechanisms. *Nature*, **408**, 936–943.

Chu,P.J., Robertson,H.M. and Best,P.M. (2001) Calcium channel γ subunits provide insights into the evolution of this gene family. *Gene*, **280**, 37–48.

Delmas,P., Brown,D.A., Dayrell,M., Abogadie,F.C., Caulfield,M.P. and Buckley,N.J. (1998) On the role of endogenous G-protein βγ subunits in N-type Ca²⁺ current inhibition by neurotransmitters in rat sympathetic neurones. *J. Physiol. (Lond.)*, **506**, 319–329.

Dolphin,A.C. (1998) Mechanisms of modulation of voltage-dependent calcium channels by G proteins. *J. Physiol. (Lond.)*, **506**, 3–11.

Freise,D. *et al.* (2000) Absence of the γ subunit of the skeletal muscle dihydropyridine receptor increases L-type Ca²⁺ currents and alters channel inactivation properties. *J. Biol. Chem.*, **275**, 14476–14481.

Gill,R.W., Hodgman,T.C., Littler,C.B., Oxer,M.D., Montgomery,D.S., Taylor,S. and Sanseau,P. (1997) A new dynamic tool to perform assembly of expressed sequence tags (ESTs). *CABIOS*, **13**, 453–457.

Hofmann,K. and Stoffel,W. (1993) TMbase—a database of membrane spanning proteins segments. *Biol. Chem. Hoppe-Seyler*, **374**, 166.

Jay,S.D., Ellis,S.B., McCue,A.F., Williams,M.E., Vedvick,T.S., Harpold,M.M. and Campbell,K.P. (1990) Primary structure of the γ subunit of the DHP-sensitive calcium channel from skeletal muscle. *Science*, **248**, 490–492.

Jones,S.W. (1998) Overview of voltage-dependent calcium channels. *J. Bioenerg. Biomembr.*, **30**, 299–312.

Kang,M.-G., Chen,C.-C., Felix,R., Letts,V.A., Frankel,W.N., Mori,Y.

and Campbell,K.P. (2001) Biochemical and piophysical evidence for γ2 subunit association with neuronal voltage-activated Ca²⁺ channels. *J. Biol. Chem.*, **276**, 32917–32924.

Klugbauer,N., Dai,S.P., Specht,V., Lacinov,L., Marais,E., Bohn,G. and Hofmann,F. (2000) A family of γ-like calcium channel subunits. *FEBS Lett.*, **470**, 189–197.

Kornau,H.C., Seeburg,P.H. and Kennedy,M.B. (1997) Interaction of ion channels and receptors with PDZ domain proteins. *Curr. Opin. Neurobiol.*, **7**, 368–373.

Lacerda,A.E., Perez-Reyes,E., Wei,X., Castellano,A. and Brown,A.M. (1994) T-type and N-type calcium channels of *Xenopus* oocytes: evidence for specific interactions with β subunits. *Biophys. J.*, **66**, 1833–1843.

Letts,V.A. *et al.* (1998) The mouse stargazer gene encodes a neuronal Ca²⁺-channel γ subunit. *Nature Genet.*, **19**, 340–347.

Meir,A., Bell,D.C., Stephens,G.J., Page,K.M. and Dolphin,A.C. (2000) Calcium channel β subunit promotes voltage-dependent modulation of α1B by Gβγ. *Biophys. J.*, **79**, 731–746.

Morales,M., Colicos,M.A. and Goda,Y. (2000) Actin-dependent regulation of neurotransmitter release at central synapses. *Neuron*, **27**, 539–550.

Perez-Reyes,E. (1998) Molecular characterization of a novel family of low voltage-activated, T-type, calcium channels. *J. Bioenerg. Biomembr.*, **30**, 313–318.

Plummer,M.R., Logothetis,D.E. and Hess,P. (1989) Elementary properties and pharmacological sensitivities of calcium channels in mammalian peripheral neurons. *Neuron*, **2**, 1453–1463.

Powers,P., Liu,S., Hogan,K. and Gregg,R. (1993) Molecular characterization of the gene encoding the γ subunit of the human skeletal muscle 1,4-dihydropyridine-sensitive Ca²⁺ channel (CACNLG), cDNA sequence, gene structure and chromosomal location. *J. Biol. Chem.*, **268**, 9275–9279.

Raghib,A., Bertaso,F., Davies,A., Page,K.M., Meir,A., Bogdanov,Y. and Dolphin,A.C. (2001) Dominant-negative synthesis suppression of voltage-gated calcium channel Ca_V2.2 induced by truncated constructs. *J. Neurosci.*, **21**, 8495–8504.

Schorge,S., Gupta,S., Lin,Z.X., McEnery,M.W. and Lipscombe,D. (1999) Calcium channel activation stabilizes a neuronal calcium channel mRNA. *Nature Neurosci.*, **2**, 785–790.

Sharp,A.H., Black,J.L.,III, Dubel,S.J., Sundarraj,S., Shen,J.P., Yunker,A.M.R., Copeland,T.D. and McEnery,M.W. (2001) Biochemical and anatomical evidence for specialized voltage-dependent calcium channel γ isoform expression in the epileptic and ataxic mouse, stargazer. *Neuroscience*, **105**, 599–617.

Swick,A.G., Janicot,M., Cheneval-Kastelic,T., McLenithan,J.C. and Lane,M.D. (1992) Promoter-cDNA-directed heterologous protein expression in *Xenopus laevis* oocytes. *Proc. Natl Acad. Sci. USA*, **89**, 1812–1816.

Tomita,S., Nicoll,R.A. and Bredt,D.S. (2001) PDZ protein interactions regulating glutamate receptor function and plasticity. *J. Cell Biol.*, **153**, 19–24.